

Misalignment and Muon Scale Corrections Extracted from the 2011A $Z \rightarrow \mu\mu$ Sample

Arie Bodek, Jiyeon Han, and Willis Sakumoto

Department of Physics and Astronomy, University of Rochester, Rochester NY, 14627 USA

Abstract

We use the 2011A Drell-Yan $\mu^+\mu^-$ data sample in the Z Mass Region ($60 < M_{\mu\mu} < 120$ GeV/c²) to obtain corrections to the reconstructed muon momentum. These corrections, extracted using a new technique, compensate for misalignments of the CMS detector. We find that the misalignments in data and Monte Carlo are different and extract corrections for both samples. The samples used for the study correspond to 2.1 fb^{-1} of integrated luminosity collected in pp Collisions at $\sqrt{s}=7$ TeV till August, 22, 2011 (referred to as the 2011A data set). The corrections to the muon momentum in both data and MC, which we refer to as the Rochester Momentum Correction, are extracted as a function of muon charge (Q), η and ϕ .

Version 2

1 Introduction

We use the 2011A Drell-Yan $\mu^+\mu^-$ data sample in the Z Mass Region ($60 < M_{\mu\mu} < 120 \text{ GeV}/c^2$) to obtain corrections to the reconstructed muon momentum to compensate for misalignments of the CMS detector. The samples used for the study correspond to 2.1 fb^{-1} of integrated luminosity collected in pp Collisions at $\sqrt{s}=7 \text{ TeV}$ till August, 22, 2011 (referred to as the 2011A data set). We use a new technique that has not been used before.

The CMS reconstruction software in both data and MC uses incorrect alignment geometries of the tracker. The misalignments in the data and the MC are different from each other. This affects the momentum determination of muons in both data and MC. The misalignment of the tracker results in a charge (Q), η , and ϕ dependence in the reconstruction of the muon momentum for both samples.

Although both data and MC samples were processed using the latest alignment geometry (as of December 2011) we find that the misalignment in the tracker is not fully accounted for. To correct for the remaining effect of misalignment, a CMS official momentum correction (MuscleFit) was developed by the tracking group. The MuscleFit correction is parametrized using Ansatz functions. The Ansatz functions should (in principle) correct for the residual charge, η , and ϕ dependence in the determination of the muon momentum. The functional forms are complicated and are different for data and MC.

The MuscleFit correction has been updated up to first 750 pb^{-1} of the 2011 data (though not approved yet) [1]. When we apply the MuscleFit correction from the first 750 pb^{-1} to the entire 2011 data set, we find that it does a poor job in correcting for misalignments (as described in an appendix to this note). There is no MuscleFit available for entire 2011 MC set. When we apply the 2010 MC MuscleFit to the 2011 MC, it also does a very poor job. We find that the MuscleFit partially corrects for misalignments in ϕ but does not correct for misalignments in η

In this note we use a new technique to extract corrections to the reconstructed muon momentum using the average of $1/p_T$ ($< 1/p_T >$) spectra of muons from Z decays. The corrections are extracted as a function of charge, η , and ϕ . We will refer to this correction as the Rochester Momentum Correction.

As we show in this communication, the Rochester Momentum Correction corrects for all of the misalignments and no MuscleFit is needed. Therefore, the Rochester Momentum Correction described in this note should be applied 2011A data without the application of any MuscleFit correction.

However, in the future, when a MuscleFit for the 2011A data becomes available, we can repeat the study and extract an updated Incremental Rochester Momentum Correction that only corrects for residual misalignment that are not fully compensated for by the (as yet to be developed 2011A) MuscleFit. In that case, analyses the would like to the MuscleFit in the future, should apply an Incremental Rochester Momentum Correction.

2 Data Set and Event Selection

For the extraction of corrections to the reconstructed muon momentum we use 2011A data set which corresponds to 2.1 fb^{-1} of integrated luminosity. We use events that pass the HLT DoubleMu_7 trigger path. The sample is produced using the CMSSW_4.2.8 version. The Jason file is required to select the runs which satisfy the good detector condition.

The MC set which is used is the $Z \rightarrow \mu\mu$ Powheg sample of Summer 11 version which includes Pythia parton showering. The analysis selection criteria are those proposed by the Vector Boson Task Force.

These are outlined in: <https://twiki.cern.ch/twiki/bin/viewauth/CMS/VbtfZMuMuBaselineSelection>.

In the definition of isolation, we use the combined track and HCAL fractional isolation defined as $(TrkIso + HadIso)_{\Delta R < 0.3}/P_T < 0.15$ (as used by the Dilepton group). If the EM energy is not included in the isolation requirement, then the momentum dependence of the efficiency is expected to be constant. Therefore, we do not include the EM energy in the definition of isolation.

Note that if the EM energy is included in the isolation requirement, then FSR photons cause in a momentum dependence of the efficiency, as well as a complicated correlation between the efficiency of the two muons.

Specifically, the selection criteria are:

- HLT DoubleMu_7
- Muon selection : VBTF muon selection is applied

- 63 • $P_t > 20 \text{ GeV}$ and detector $|\eta| < 2.4$
- 64 • Global and Tracker Muon
- 65 • Combined relative isolation : $(TrkIso + HadIso)_{\Delta R < 0.3} / P_T < 0.15$
- 66 • Global muon normalized fit $\chi^2 < 10$
- 67 • Number of Tracker hits greater than 10
- 68 • Number of pixel hits greater than or equal to 1
- 69 • Number of muon stations greater than or equal to 2
- 70 • $dxy < 0.2$
- 71 • Mass selection : $60 < Mass < 120 \text{ GeV}/c^2$

72 The muon reconstruction efficiency as a function of η is extracted from the data. An efficiency scale factor obtained
 73 from the data is applied to the MC to correct for the difference of the efficiency between data and MC.

74 3 Reference Plots Used in the Muon Momentum Study

75 A misalignment of the tracker generates distortions in several kinematic distributions of Drell-Yan ($Z/\gamma^* \rightarrow \mu\mu$)
 76 events in the Z boson mass region. Since the misalignment of data and MC are different, the distributions will be
 77 distorted in different ways for data and MC. Detector misalignment results in the following:

- 78 • It is responsible for charge (Q), η , and ϕ dependence of the reconstructed Z boson mass. The expected Z
 79 boson mass is known from the generated (post FSR) spectrum in MC.
- 80 • It yields difference in the overall shape of the Z mass distributions between the data and MC (if data and
 81 MC have different misalignments). A difference in shape will also occur if the detector resolution in the MC
 82 is not modeled correctly.
- 83 • A charge dependence in the reconstructed muon momentum creates unphysical wiggles in the forward and
 84 backward charge asymmetry (A_{fb}) of Drell-Yan events as a function of dilepton mass (in the region of the
 85 Z peak). This yields one of two powerful checks on a difference in the momentum scale between positive
 86 and negative muons.
- 87 • In the low Z boson P_T region ($P_T < 10 \text{ GeV}/c$), the ϕ distribution in the Collins-Soper frame (CS) [3],
 88 ϕ_{CS} , is expected to be flat. However, resolution smearing in the muon momentum creates an excess around
 89 $\phi_{CS} = 0$ and $\pm\pi$ in the reconstructed level ϕ_{CS} . The level of the excess at $\phi_{CS} = 0$ and $\pm\pi$ is expected
 90 to be the same if the muon momentum scales and resolutions are the same between μ^+ and μ^- . Therefore,
 91 ϕ_{CS} distribution in low Z P_T region provides the second powerful check on a difference in the momentum
 92 scale between positive and negative muons. A simple way to think about this is as follows: ϕ_{CS} is the angle
 93 between the direction of the Z boson P_T and the direction of the positive lepton. For Z $P_T = 0$ there is no
 94 preferred x axis. However, if the calibration of the positive and negative muons are different, $P_T = 0$ events
 95 end up with a Z P_T along either the positive or the negative muon direction in ϕ_{CS}

96 In our study we use the following kinematic distributions as reference plots to test the validity of the momentum
 97 corrections.

- 98 • The overall dimuon invariant mass spectrum ($M_{\mu^+\mu^-}$).
- 99 • A_{fb} as a function of mass.
- 100 • ϕ_{CS} in two Z P_T bins: $0 < P_T < 5 \text{ GeV}/c$, and $5 < P_T < 10 \text{ GeV}/c$.
- 101 • A comparison of the Z P_T spectrum between data and MC.
- 102 • The average Z mass as a function of ϕ of either the μ^+ or the μ^-

- 103 • The average Z mass as a function of η of either the μ^+ or the μ^- .
- 104 • We use the same procedure to extract the corrections for data and MC. Since for the MC we know the
- 105 generated muon momentum, we can use the generated information in the MC sample as an additional check
- 106 on the procedure.

107 Figure 1 and 2 show the reference plots before the application of any muon momentum correction to either data or
 108 MC. Figure 3 shows the Z mass profile in $60 < M < 120 \text{ GeV}/c^2$ mass range as a function of μ^- and μ^+ in the
 109 generator level before the photon radiation effect (FSR). The Z boson has the forward and backward asymmetry
 110 (A_{fb}), which results on the asymmetry in the Z mass profile plot for μ^- and μ^+ . This effect is shown in the plot
 111 in the right side of Figure 3 (black vs. red points).

112 The following features are observed in Fig. 1:

- 113 • The top two plots indicate that the location of the Z peak in mass is incorrect and the shape of the data in
 114 mass is different from the MC.
- 115 • The left middle plot shows unphysical wiggles in A_{fb} in both data and MC, indicating that the momentum
 116 scales for positive and negative muons are different in both data and MC
- 117 • The right middle plot shows that the MC does not have the correct P_T spectrum.
- 118 • The bottom two plots show that the MC does not have the correct P_T spectrum (level) and that the momentum
 119 scales for positive and negative muons are different (the peaks at $\phi_{CS} = 0$ and $\pm\pi$ have different heights).

120 The following features are observed in Fig. 2:

- 121 • The top two plots show that the average Z mass depends on ϕ (it should be independent of ϕ). They also
 122 show that the momentum scales for positive and negative muons are different in both data and MC, and the
 123 difference is a function of ϕ of the muon.
- 124 • The bottom two plots show that the η dependence of the muon momentum scales in data and MC are
 125 different.

126 4 Muon Momentum Correction- First Iteration

127 To correct for the effect of track misalignments, we extract a correction to the reconstructed muon momentum
 128 which is a function of charge (Q), η , and ϕ of the muon.

129 The procedure is to require that the mean of $1/p_T$ ($< 1/p_T >$) of muons in data (reconstructed) and MC (recon-
 130 structed) in bins of Q , η , and ϕ should each be equal to the mean $< 1/p_T >$ of the MC at the generated level (in a
 131 specific Q , η , and ϕ bin). Since the Z mass is known, and the P_T spectrum in MC can be tuned to agree with the
 132 data, this procedure yields an absolute calibration of the momentum scale.

133 In general, an overall momentum scale (e.g. error in the B field) should be the same for positive and negative
 134 muons. A misalignment would results in a difference in the mean $< 1/p_T >$ between positive and negative muon.
 135 A muon momentum correction that corrects for a misalignment is additive in $1/p_T$.

136 As discussed later in this note, we find that the momentum correction originates from misalignment and is therefore
 137 additive in $1/p_T$. After applying the additive $1/p_T$ momentum correction, we apply overall scale factors to the MC
 138 (which are common to positive and negative muons) to match the Z peak positions and width in data and MC..

139 The correction factor, $C^{Data/MC}(Q, \eta, \phi)$, is defined as the difference in the mean $< 1/p_T >$ between the mean
 140 $< 1/p_T >$ for the MC at the generated level and reconstructed data (or reconstructed MC). This is done in bins
 141 of Q , η and ϕ . The correction factor, $C^{Data/MC}(Q, \eta, \phi)$, is reorganized to consider two different effect, muon
 142 momentum scale from B-field effect and the misalignment effect. The muon momentum difference from B-field
 143 effect has no charge dependence, but p_T dependence and this can be corrected by the multiplicative correction.
 144 The muon momentum difference from the misalignment effect has the charge dependence, so this effect has the
 145 opposite sign of the correction for μ^+ and μ^- and it is corrected by the additive correction. We define the correction
 146 factor for the B-field effect ($D_m = (C^{Data/MC}(+, \eta, \phi) + C^{Data/MC}(-, \eta, \phi))/2.0$) and the misalignment effect
 147 ($D_a = (C^{Data/MC}(+, \eta, \phi) - C^{Data/MC}(-, \eta, \phi))/2.0$)

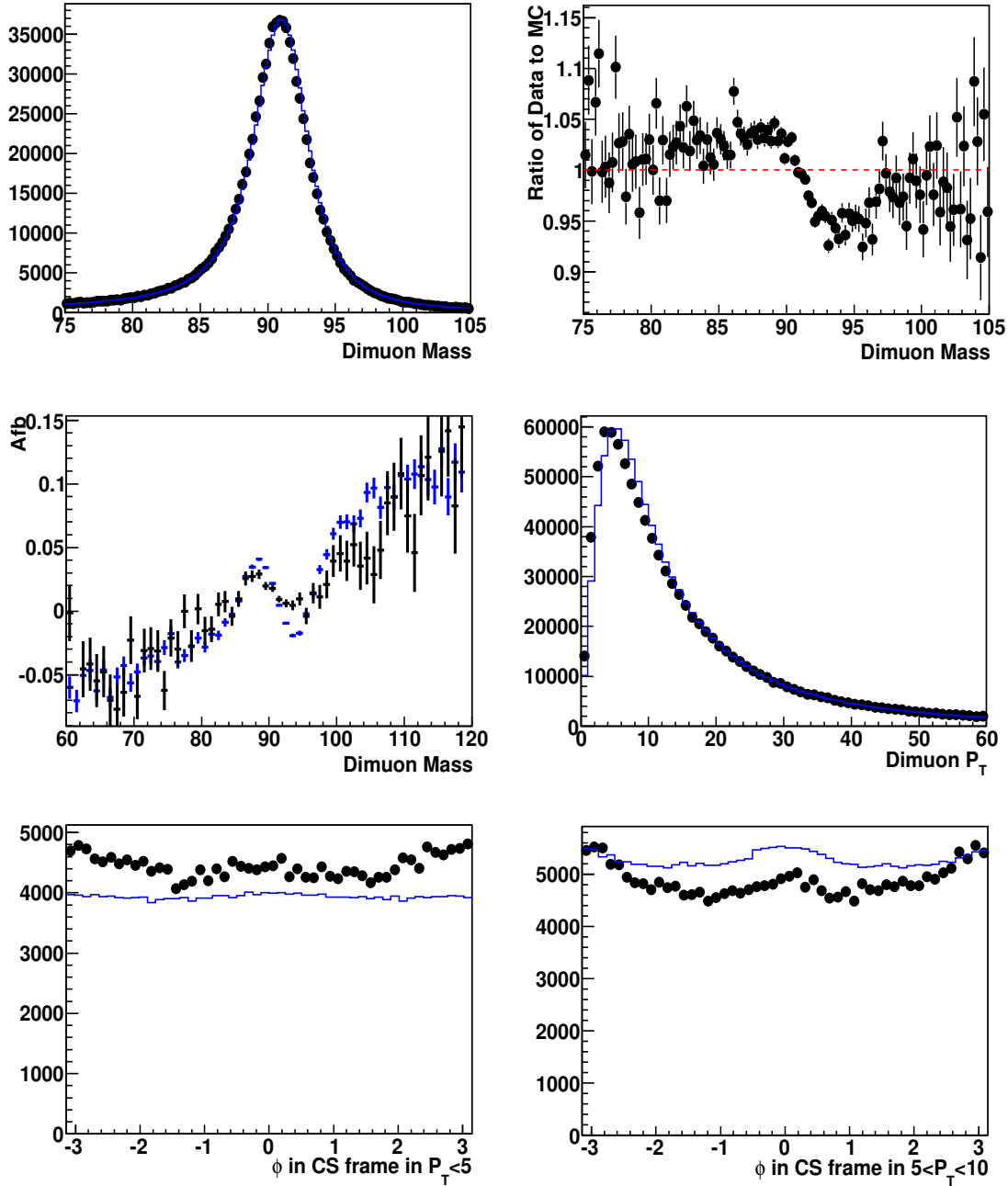


Figure 1: Reference plots BEFORE any corrections. Top Plots: Comparison of the dimuon invariant mass distribution between the data (black) and MC (blue) (left), and the ratio of data to MC (right). Middle plots: Comparison of A_{fb} as a function of mass (left) and boson P_T distribution (right) between the data (black) and MC (blue). Bottom plots: Comparison of ϕ in the Collins-Soper frame for boson $P_T < 5 \text{ GeV}/c$ (left), and ϕ in the Collins-Soper frame for boson $5 < P_T < 10 \text{ GeV}/c$ (right) for data (black) and MC (blue). The plots are normalized to the total number of events of the data in the $60 < M_{\mu\mu} < 120 \text{ GeV}/c^2$ mass range. (a) The top two plots indicate that the location of the Z peak in mass is incorrect and the shape of the data in mass is different from the MC. (b) The left middle plot shows unphysical wiggles in A_{fb} in both data and MC, indicating that the momentum scales for positive and negative muons are different in both data and MC (c) The right middle plot shows that the MC does not have the correct P_T spectrum. (d) The bottom two plots show that the MC does not have the correct P_T spectrum (level) and that the momentum scales for positive and negative muons are different (the peaks at $\phi_{CS} = 0$ and $\pm\pi$ are different).

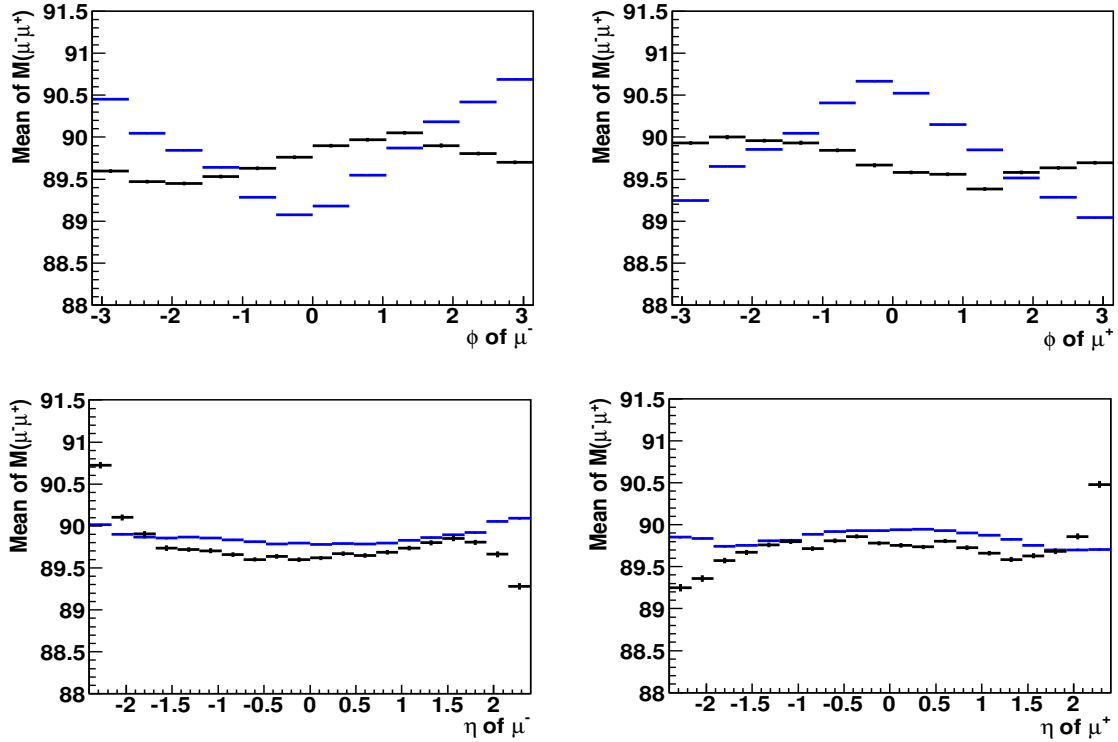


Figure 2: Reference plots BEFORE any corrections: Top Plots: Comparison of the average of $M_{\mu\mu}$ as a function of ϕ for μ^- (left) and the average of $M_{\mu\mu}$ as a function ϕ for μ^+ (right) between the data (black) and MC (blue). Bottom Plots: Comparison between the data (black) and MC (blue) of the average of $M_{\mu\mu}$ as a function of η for μ^- (left) and the average of $M_{\mu\mu}$ as a function of η for μ^+ (right). The top two plots show that the average Z mass depends on ϕ (it should be independent of ϕ). They also show that the momentum scales for positive and negative muons are different in both data and MC, and the difference is a function of ϕ of the muon. The bottom two plots show that the η dependence of the muon momentum scales in data and MC are different.

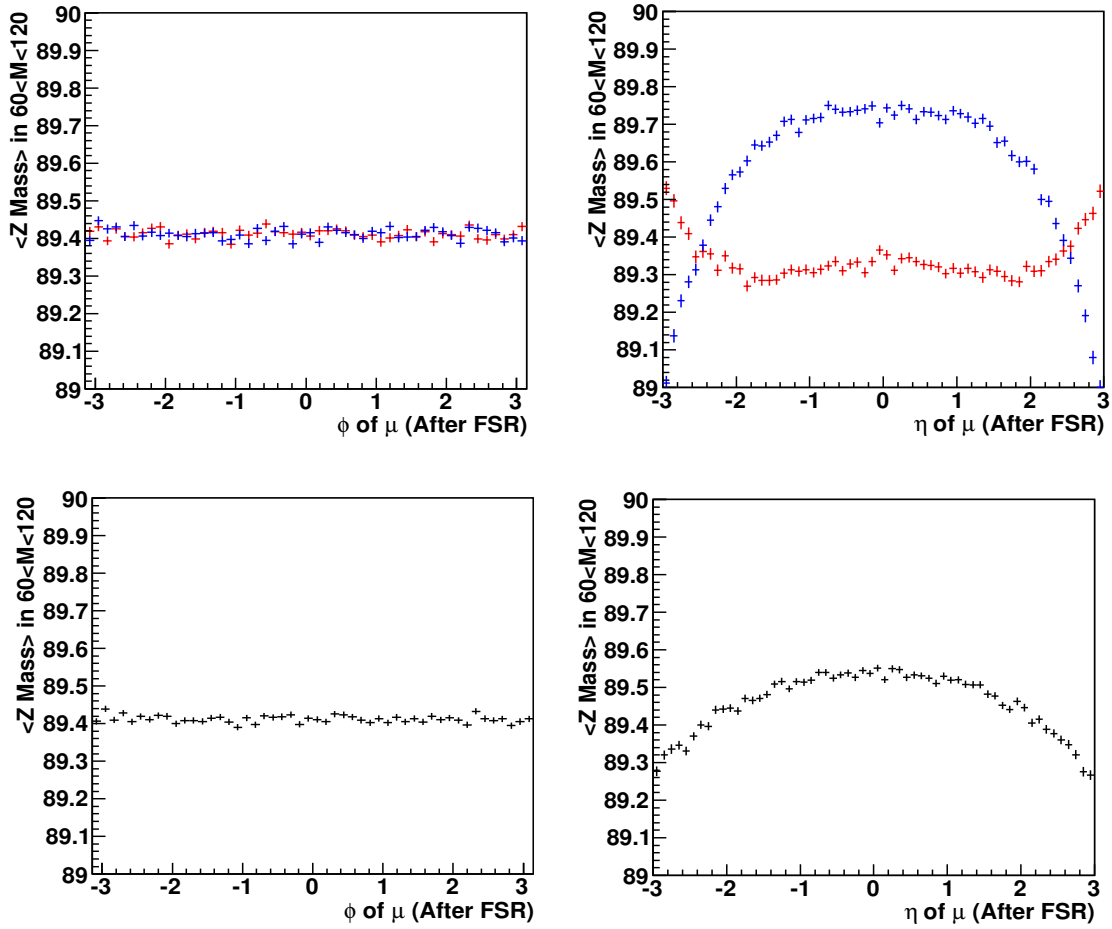


Figure 3: Z mass profile plot as a function of ϕ (left) and η (right) of μ in the generator level. Top plot : Z mass profile plot as a function of ϕ (left) and η (right) of μ^- (red points) and μ^+ (blue points) in the generator level without any selection after the photon radiation effect (FSR). Bottom plot : Z mass profile plot as a function of ϕ (left) and η (right) of μ (black points) in the generator level without any selection after the photon radiation effect (FSR). The mass window, $60 < M < 120 \text{ GeV}/c^2$, is used to get the mean of the Z mass ($y - axis$).

$$C^{Data/MC}(Q, \eta, \phi) = \langle 1/p_T^{MC(gen.)}(Q, \eta, \phi) \rangle - \langle 1/p_T^{Data/MC(rec.)}(Q, \eta, \phi) \rangle \quad (1)$$

$$D_m(\eta, \phi) = (C^{Data/MC}(+, \eta, \phi) + C^{Data/MC}(-, \eta, \phi))/2.0 \quad (2)$$

$$D_a(\eta, \phi) = (C^{Data/MC}(+, \eta, \phi) - C^{Data/MC}(-, \eta, \phi))/2.0 \quad (3)$$

$$\frac{1}{p_{T,corrected}^{\pm}} = \frac{1}{p_T^{\pm}} \times (1.0 + D_m(\eta, \phi)/\langle 1/p_T^{\pm} \rangle) \pm D_a(\eta, \phi) \quad (4)$$

148 where, MC(rec.) and MC(gen.) labels the information on the muon momentum for the MC at the reconstructed
 149 and generated levels, respectively. The $C^{Data/MC}$ is the muon momentum correction factor for the data or MC
 150 in bins of Q , η , and ϕ of the muon (8×8 matrix in η and ϕ for each muon polarity). This $\langle 1/p_T \rangle$ correction
 151 corrects for the charge, η , and ϕ dependence of the mis-reconstructed momentum.

152 Figure 4 and 5 show the $\langle 1/p_T \rangle$ correction for the data and for the MC ($C^{Data/MC}(Q, \eta, \phi)$).

153 After applying the $\langle 1/p_T \rangle$ additive correction, we apply global scale factors to the MC to match the Z mass
 154 position, and momentum resolutions in data and MC. The three global factors, T, Δ , and SF, are estimated by
 155 comparing the overall $M_{\mu^+\mu^-}$ mass distributions between data and MC (using a χ^2 test). These global scale
 156 factors are only applied to the MC. They are define by the following equations (which are also used at CDF):

$$p_i^{corrected} = p_i + T \times (p_i^{gen.} - p_i) \quad (5)$$

$$\frac{1}{p_T^{corrected}} = \frac{1}{p_T} + \Delta \times Random :: Gaus(1, SF) \quad (6)$$

157 where p_i is the reconstructed muon momentum in MC ($i = x, y, \text{ and } z$) and $p_i^{gen.}$ is the generated muon momentum
 158 in MC.

159 Figure 6 shows χ^2 distributions for the comparison of data to MC as a function each global scale factor. The
 160 measured global factors (extracted from the χ^2 plot) are summarized in Table 1. Here T is the factor that increases
 161 the resolution in σ_{P_T} in MC to better agree with the data (by about 5%). Δ is a correction for the overall momentum
 162 scale (the P_T of muons from Z decays is of order 30 GeV, $1/P_T \approx 3 \times 10^{-5}$. Therefore, $\Delta \approx 6 \times 10^{-5}$ is a
 163 shift of about 1.8 %). The parameter SF is an additional resolution smearing in $1/P_T$ ($SF\Delta \approx 5 \times 10^{-5}$, which
 164 increases the resolution in $1/P_T$ in the MC by about 1.8 %).

165 After all correction, the Z peak in the reconstructed level of data and MC is 90.76 GeV/ c^2 , which is lower than the
 166 Z mass of the generated level after FSR, 91.06 GeV/ c^2 after kinematic cuts ($P_T > 20$ GeV and $|\eta| < 2.4$ for both
 167 muons). (Z mass peak is obtained by fitting Z mass region using Breit-Wigner function.) To set the Z mass to
 168 the input Z mass after FSR, we apply the extra global factor, $G = 1.003 \pm 0.001$.

Table 1: Iteration 1: Global scale factors (T, Δ , and SF) for the in the MC. The global factors are determined by
 comparing the $M_{\mu^+\mu^-}$ distributions in data and MC. These factors are applied only to the MC. Here T is a factor
 that scales the resolution in MC to better agree with the data. Δ is a correction for the overall momentum scale,
 and SF is an additional resolution smearing in $1/P_T$.

Global Factor	Value
T	-0.0480 ± 0.0035
Δ	$(6.4488 \pm 0.0789) \times 10^{-5}$
SF	0.8179 ± 0.1457
G	1.003 ± 0.001

169 Figure 7 shows the reference plots after applying the iteration 1 correction factors, $C(Q, \eta, \phi)$, T, Δ , and SF. The
 170 reference plots shows better agreement between the data and MC. The unphysical wiggles in the A_{fb} distributions
 171 in both data and MC are no longer there, and the peaks at $\phi_{CS} = 0$ and $\pm\pi$ are of equal magnitude. However, the
 172 middle plot shows that Z P_T distribution in MC do not agree with the data. This results in offsets between data
 173 and MC in the ϕ_{CS} distributions for the two Z P_T ranges. (The distributions are normalized to the total number
 174 of events in data for $60 < M_{\mu^+\mu^-} < 120$ GeV/ c^2 mass window.)

175 The disagreement [5] between data and MC for the $Z P_T$ distribution at low P_T implies that the Powheg MC
 176 generator with Pythia parton showering (used in CMS) should be tuned. In order to get better agreement between
 177 the data and MC, we apply a $Z P_T$ correction shown in Figure 8 to the MC at the generator level such that it
 178 matches the data.

179 The $Z P_T$ correction removes the discrepancy in the overall levels in the comparison of ϕ_{CS} distributions between
 180 the data and MC for the two low P_T ranges. Figure 9, 10, and 11 show the reference plots after applying both
 181 the momentum correction and the additional $Z P_T$ correction in MC. With the additional $Z P_T$ correction, there is
 182 agreement in the ϕ_{CS} distributions between data and MC. After all correction, we compare the p_T distribution of
 183 μ^- and $m\mu^+$ between data and MC shown in Figure 12.

Table 2: Iteration 2 (final) : The global scale factors (T, Δ , and SF) for additional muon momentum correction in the MC. The global factors are determined by comparing the $M_{\mu^+\mu^-}$ distributions in data and MC. These factors are applied only to the MC. Here T is a factor that scales the resolution in MC to better agree with the data. Δ is a correction for the overall momentum scale, and SF is an additional resolution smearing in $1/P_T$.

Global Factor	Value
T	-0.0474 ± 0.0037
Δ	$(3.3359 \pm 0.0786) \times 10^{-5}$
SF	1.2555 ± 0.3340
G	1.0020 ± 0.0001

184 5 Muon Momentum Correction- Final Iteration

185 Now that the $Z P_T$ in the Powheg MC generator has been tuned to match the data, we repeat our analysis, and
 186 extract updated muon momentum corrections. This is the second and final iteration.

187 Figure 13 and 14 show the $\langle 1/p_T \rangle$ muon correction factors for the data and MC in the final iteration. The
 188 momentum corrections in the final iteration are very close to the corrections extracted in the first iteration.

189 Figure 6 shows the χ^2 distribution for the global factors, T, Δ , and SF for the final iteration. The global factors T,
 190 Δ , SF, and G for the final iteration are given in Table 2.

191 Figure 16, 17, and 18 show the reference plots after all corrections for the final iteration, and Figure 19 shows the
 192 p_T distribution of the muon after all corrections for the final iteration.

193 6 Conclusion

194 Using the Drell-Yan dimuon sample, we extract corrections to the reconstructed muon momentum that originate
 195 from tracking misalignments. The corrections are obtained by using the average $\langle 1/p_T \rangle$ of muon in bins of
 196 charge, η , and ϕ in conjunction with the dimuon invariant mass distributions. Corrections are extracted for both
 197 data and MC.

198 The $M_{\mu^+\mu^-}$, A_{fb} , ϕ_{CS} distributions are used as reference plots to test the procedure. After the application of
 199 the muon momentum correction, the reconstruction bias which is a function of charge, η , and ϕ is removed. All
 200 kinematic distributions which are used as reference plots show good agreement between the data and MC. The
 201 offline code for the muon momentum corrections (referred to as the Rochester Momentum Correction) is now
 202 available.

203 7 Appendix

204 7.1 Test of the MuscleFit Correction

205 In this appendix, we show that the MuscleFit correction does a poor when applied to the 2011 data and MC.

206 The MuscleFit correction was the standard method to correct the muon momentum bias in 2010. However, the
 207 MuscleFit correction is not yet available for full 2011A data set.

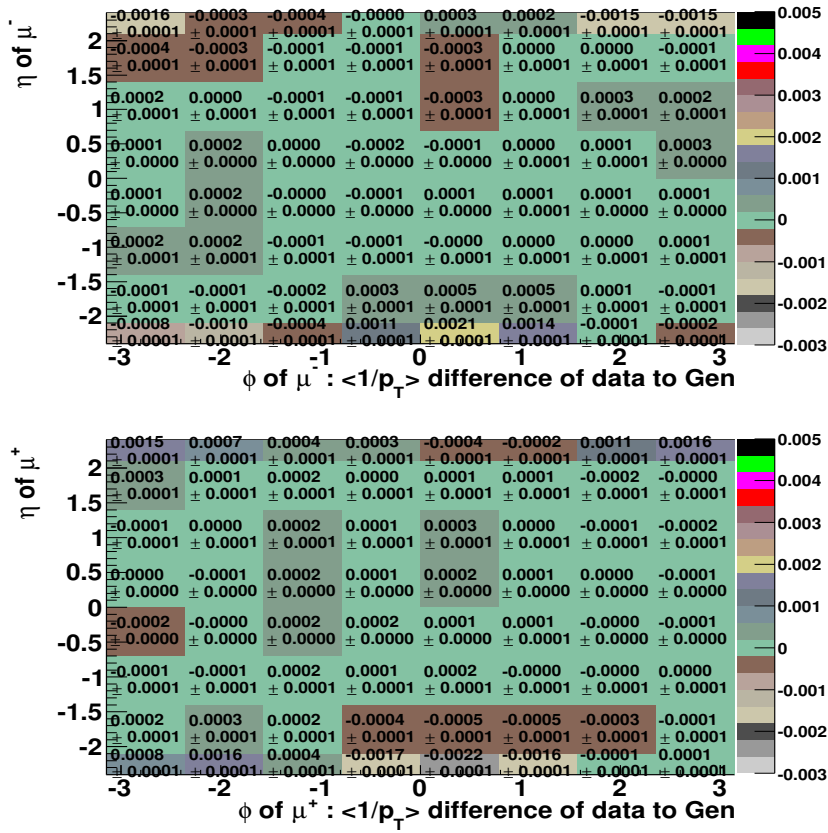


Figure 4: Iteration 1 for Data: The $\langle 1/p_T \rangle$ correction for data for μ^- (top) and μ^+ (bottom) in η and ϕ (for iteration 1).

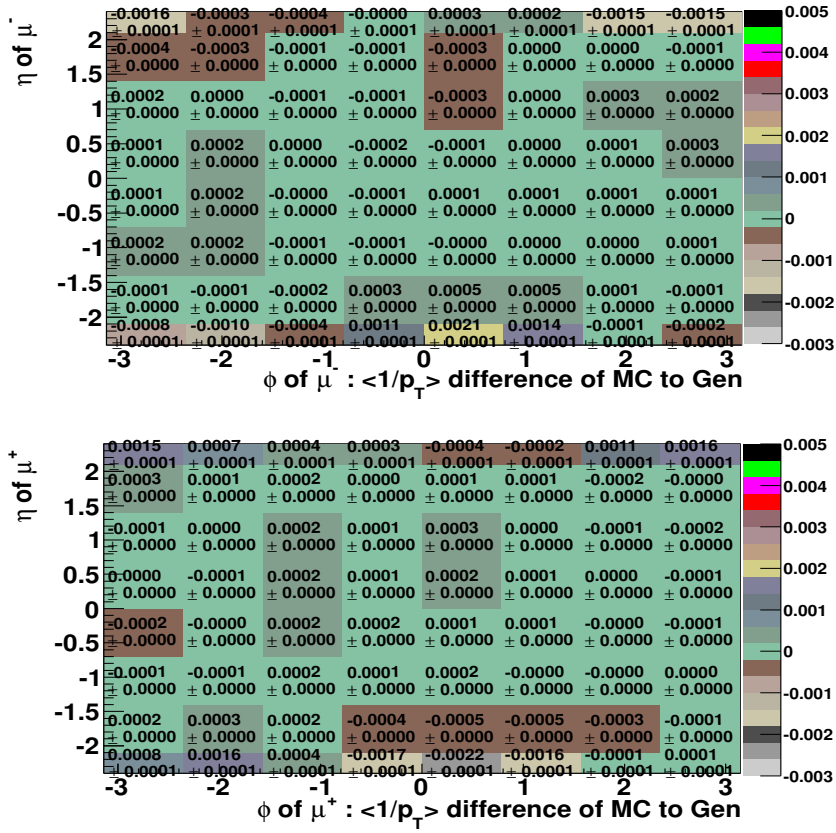


Figure 5: Iteration 1 for MC: The $\langle 1/p_T \rangle$ correction for MC for μ^- (top) and μ^+ (bottom) in η and ϕ .

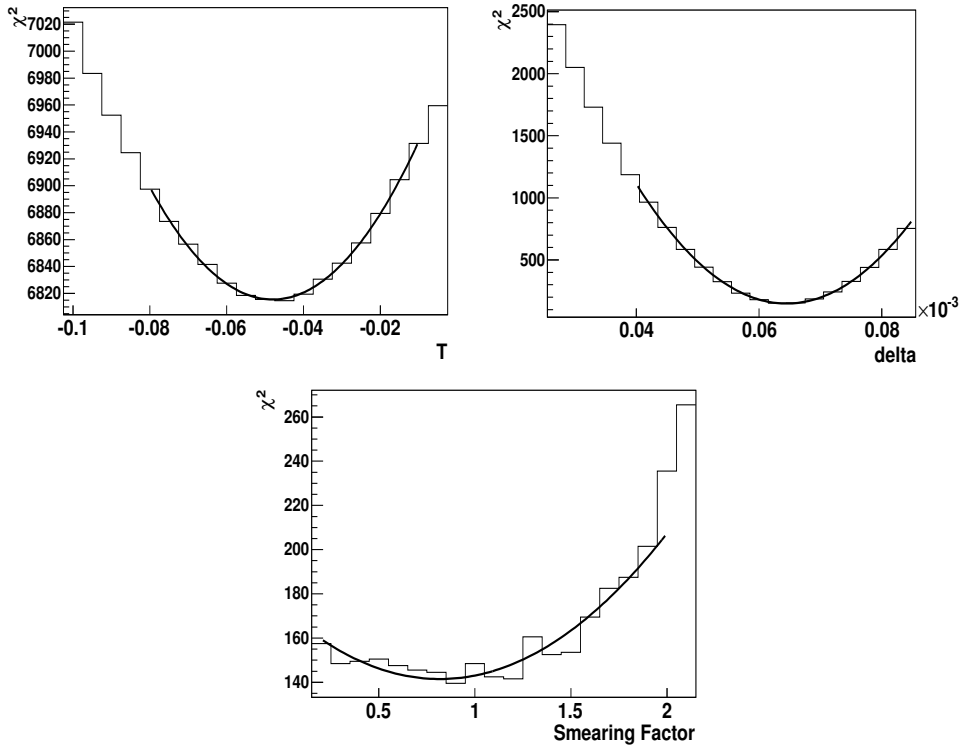


Figure 6: Iteration 1: Top Plots: χ^2 distribution as a function of the global factor, T (left) and Δ (right). Bottom Plots: χ^2 distribution as a function of the global factor, SF.

208 The MuscleFit has been updated up to first 750 pb^{-1} of the 2011A data set [1]. It is not available for the rest of
 209 the 2011A data.

210 No MuscleFit is available for the 2011A Monte Carlo . However MuscleFits for both data and MC are available
 211 for the 2010 samples.

212 As a test, we apply the MuscleFit for first 750 pb^{-1} of the 2011A data set to the entire 2011A data set, and apply
 213 the MuscleFit for the 2010 MC version to the 2011A MC.

214 To test the performance of the MuscleFit, we use the reference plots which are described in Sec. 3. Figure 20 and
 215 21 show the reference plots for the data and Figure 22 and 23 show the reference plots for MC before (black) and
 216 after (blue) applying the MuscleFit corrections.

217 After applying MuscleFit for 750 pb^{-1} of the 2011A into the data, we still have ϕ and η dependence of the
 218 muon momentum and it does not change the other kinematic distributions. The MuscleFit for MC shifts the mass
 219 distribution by $\sim 0.1 \text{ GeV}/c^2$. In addition, MC with MuscleFit still has the wiggles around Z peak region in A_{fb}
 220 and still has ϕ and η dependence of the muon momentum slightly.

221 With the MuscleFit correction we still see unphysical wiggles in A_{fb} (in both data and MC) which indicates mis-
 222 calibration between positive and negative muons in both samples. In addition, the peaks in the $\phi(\text{CS})$ in the data
 223 are not equal in height, which also indicates that there is a mis-calibration between positive and negative muons in
 224 the data.

225 The 2010 MC (2010 November version) has the different alignment scenario than the 2011A MC (2011 Spring
 226 version). Therefore, the MuscleFit for 2010 November version of MC might not work for 2011 Spring version of
 227 the MC. We find that this is indeed the case.

228 We conclude the MuscleFit from the first third of the 2011A data is applied to the full 2011A data set, it improves
 229 the ϕ dependence of the muon momentum, but does not remove the distortions in A_{fb} , or ϕ_{CS} distribution. In
 230 addition, it does not account for the η dependence of the momentum correction.

231 This study will be repeated when the updated MuscleFit parameters for full 2011A data set (for both data and
 232 MC) become available. If using the MuscleFit is desirable, we will repeat the study and extract an Incremental

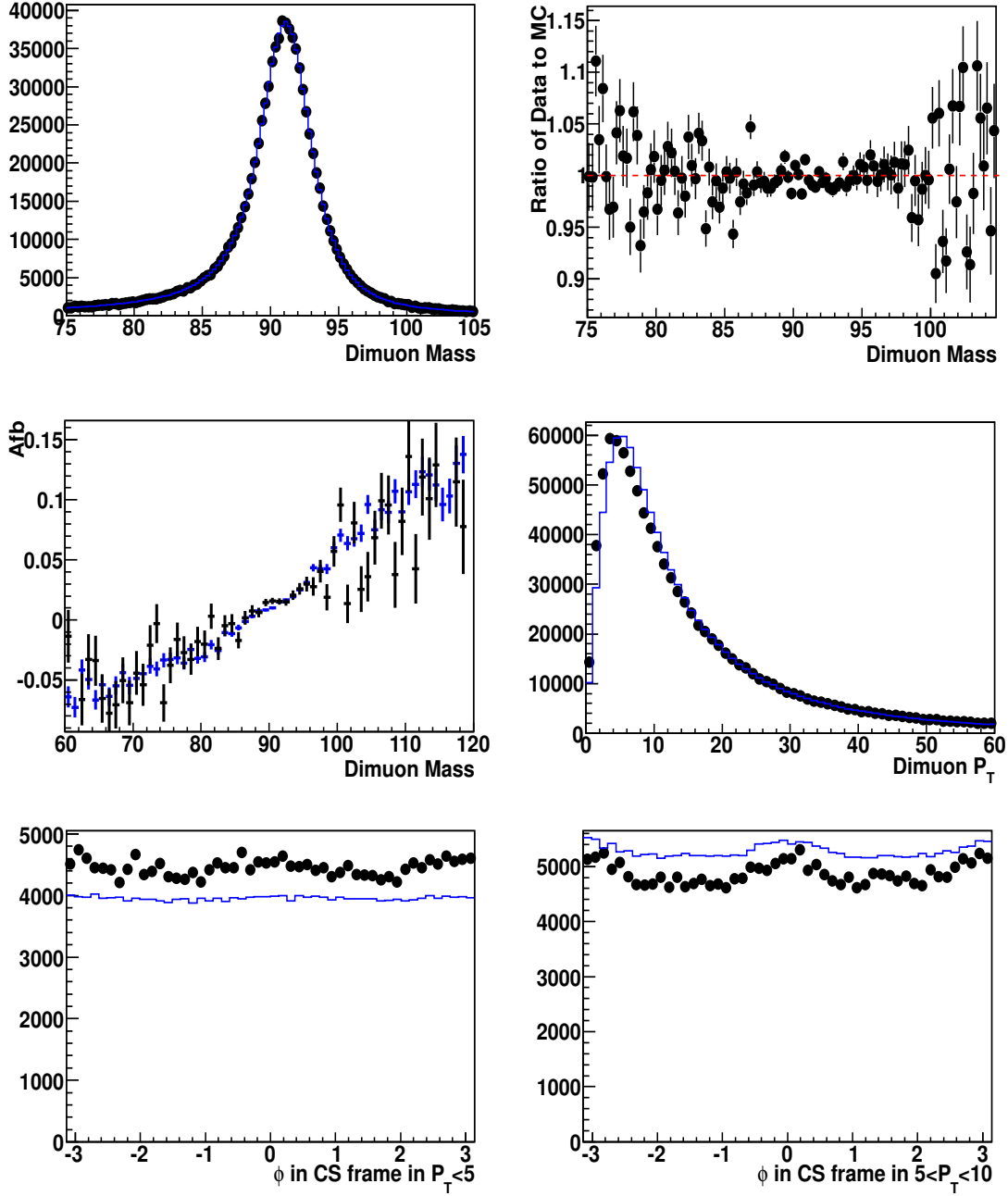


Figure 7: The reference plots ($M_{\mu^+\mu^-}$, A_{fb} , $Z P_T$, and ϕ_{CS}) after the application of the iteration 1 muon additive momentum correction. Top Plots: Comparison of the dimuon invariant mass distribution between the data (black) and MC (blue) (left) and its ratio of data to MC (right). Middle plots: Comparison of A_{fb} (left) and boson P_T (right) distributions between the data (black) and MC (blue). Bottom plots: Comparison of ϕ in the Collins-Soper frame in boson $P_T < 5$ GeV/c (left) and ϕ in the Collins-Soper frame in boson $5 < P_T < 10$ GeV/c (right) distributions between the data (black) and MC (blue). The plots are normalized to the total number of events of the data in $60 < M_{\mu\mu} < 120$ GeV/c².

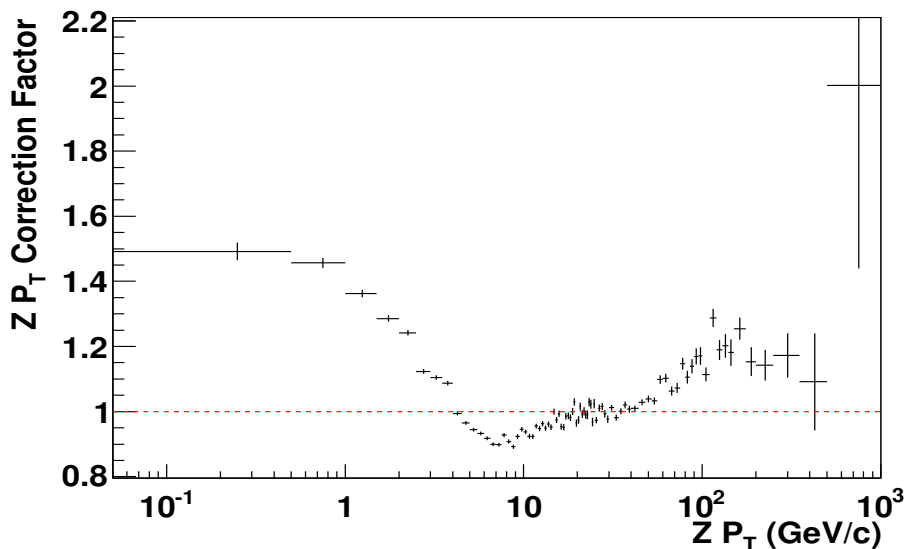


Figure 8: The $Z P_T$ correction applied to the MC at the generated level. The correction factor is obtained comparing $Z P_T$ spectrum between the data and MC after iteration 1.

233 Rochester Momentum Corrections should account for the residual mis-alignments that are not fully corrected for
 234 in the future MuscleFit.

235 7.2 Test of Momentum in High Mass Region

236 We study the muon momentum scale using the events in Z mass region, $60 < M_{\mu^+\mu^-} < 120 \text{ GeV}/c^2$. The muon
 237 momentum scale is used for not only Z mass region, but also the high mass region (muons in very high P_T region).
 238 Therefore, we test how the momentum scale works in the high momentum region. To test the muons in the high
 239 momentum region, we select the events in high mass, $M_{\mu^+\mu^-} > 250 \text{ GeV}/c^2$ and compare the average of $1/p_T$,
 240 $\langle 1/p_T \rangle$, in the reconstructed level to the average of $1/p_T$ in the generated level as a function of charge, η , and
 241 ϕ using MC. The difference of $\langle 1/p_T \rangle$ between the reconstructed and the generated level is close to be zero
 242 within 1 statistical deviation in all charge, η , and ϕ . Figure 24 shows the difference of $\langle 1/p_T \rangle$ between the
 243 reconstructed and the generated level in Z mass, $60 < M_{\mu^+\mu^-} < 120 \text{ GeV}/c^2$, and the high mass, $M_{\mu^+\mu^-} > 250$
 244 GeV/c^2 .

245 References

- 246 [1] MuscleFit for 2011A data set : Presentation in CMS Muon POG Meeting (July. 11th, 2011). The presentation
 247 is linked at <https://indico.cern.ch/getFile.py/access?contribId=1&resId=0&materialId=slides&confId=128936>.
- 248 [2] For the most recent version of POWHEG. See Simone Alioli, Paolo Nason, Carlo Oleari, Emanuele Re,
 249 arXiv:1009.5594v1 (2010). earlier versions are discussed in JHEP 0807:060,2008. NSF-KITP-08-74, May
 250 2008. 35pp. e-Print: arXiv:0805.4802 [hep-ph]
- 251 [3] J. C. Collins and D. E. Soper, Phys. Rev. D **16**, 2219 (1977). The CS frame is the center of mass of the γ^*/Z ,
 252 where the z axis is defined as the bisector of the p and \bar{p} beams. The polar angle is defined as the angle of the
 253 positive lepton with respect to the proton direction.
- 254 [4] CMS collaboration, "Search for Resonances in the Dimuon Mass Distribution in pp collisions at $\sqrt{s} = 7 \text{ TeV}$ ",
 255 CMS PAS EXO-10-013 (2010).
- 256 [5] J.G., G.P., D.G., K.K., N.K. (Northeastern University), "Measurement of the $Z/\gamma^* \rightarrow \mu^+\mu^-$ transverse mo-
 257 mentum distribution in pp collisions at $\sqrt{s} = 7 \text{ TeV}$ ", CMS note - Archive ID: 30523M

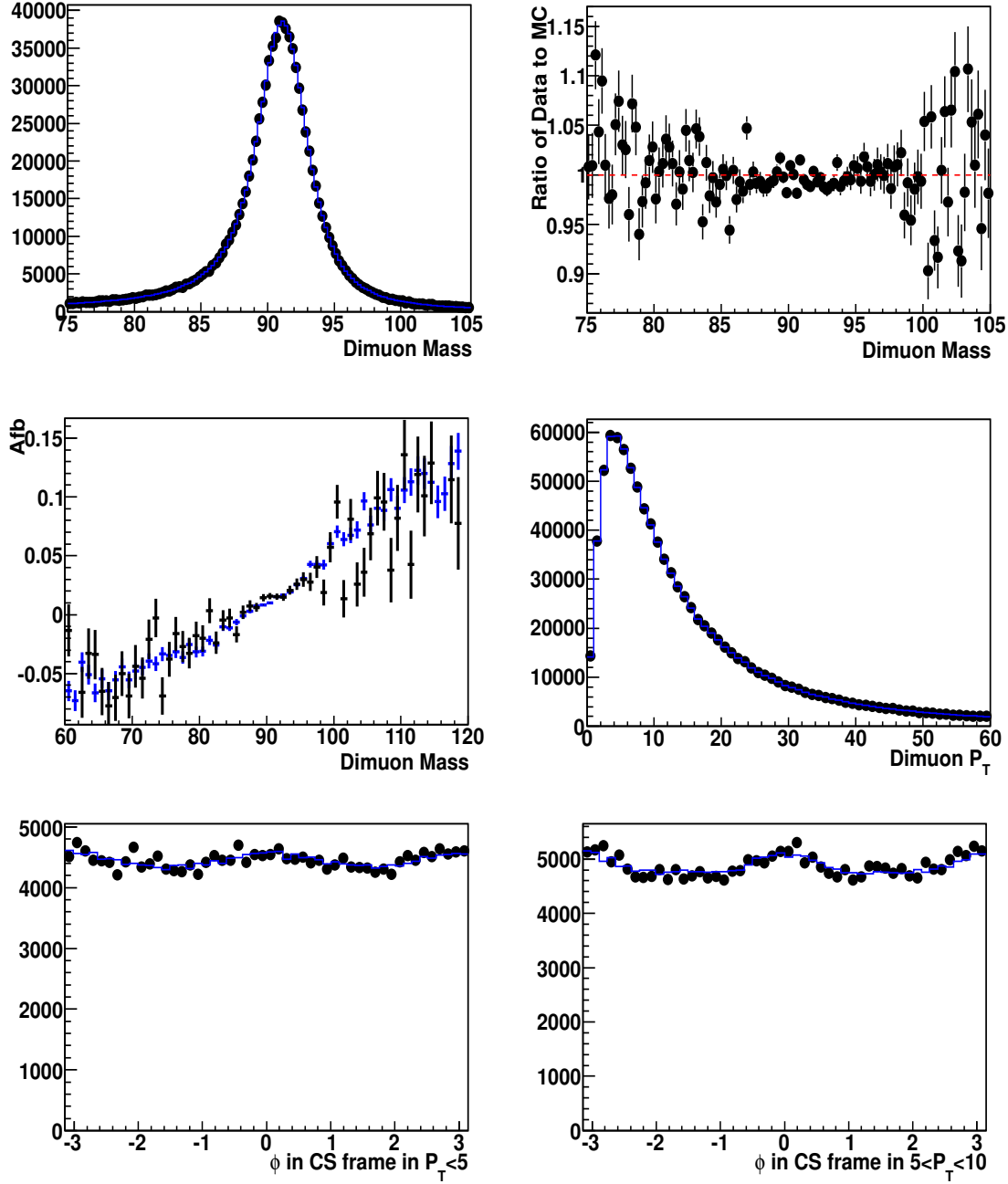


Figure 9: Iteration 1: The reference plots ($M_{\mu^+\mu^-}$, A_{fb} , $Z P_T$, and ϕ_{CS}) after iteration 1 additive muon momentum correction and $Z P_T$ correction. Top Plots: Comparison of the dimuon invariant mass distribution between the data (black) and MC (blue) (left) and its ratio of data to MC (right). Middle plots: Comparison of A_{fb} (left) and boson P_T (right) distributions between the data (black) and MC (blue). Bottom plots: Comparison of ϕ in the Collins-Soper frame in boson $P_T < 5 \text{ GeV}/c$ (left) and ϕ in the Collins-Soper frame in boson $5 < P_T < 10 \text{ GeV}/c$ (right) distributions between the data (black) and MC (blue). The plots are normalized to the total number of events of the data in $60 < M_{\mu\mu} < 120 \text{ GeV}/c^2$.

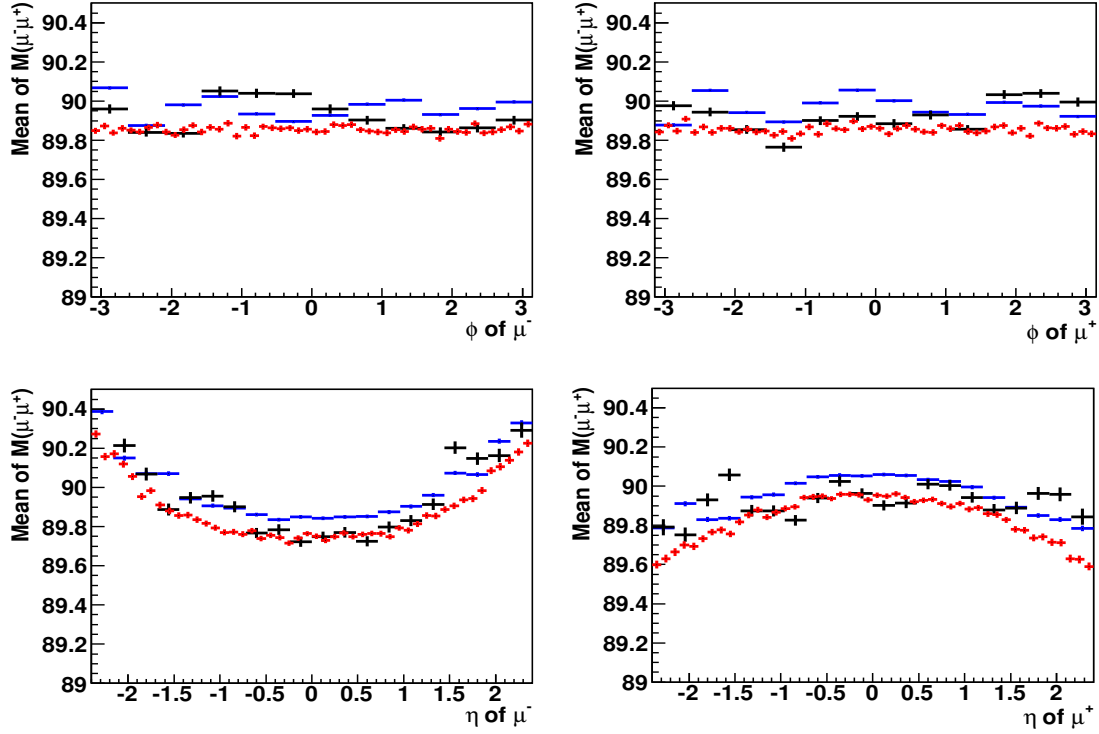


Figure 10: The $M_{\mu^+\mu^-}$ profile plot as a function of η and ϕ of μ^+ and μ^- after applying the the iteration 1 muon momentum additive correction. Top Plots: Comparison of the average of $M_{\mu\mu}$ in ϕ of μ^- (left) and the average of $M_{\mu\mu}$ in ϕ of μ^+ (right) between the data (black) and MC (blue). Bottom Plots: Comparison of the average of $M_{\mu\mu}$ in η of μ^- (left) and the average of $M_{\mu\mu}$ in η of μ^+ (right) between the data (black) and MC (blue). The red points are the $M_{\mu\mu}$ profile plot as a function of ϕ and η for μ^+ and μ^- . The peak of $M_{\mu\mu}$ in data and MC is matched to be $M_{\mu\mu}$ of the generated level after the kinematic selections ($P_T > 20 \text{ GeV}$ and $|\eta| < 2.4$ for both muons), but the mean of $M_{\mu\mu}$ in the generated level is smaller than the reconstructed level because of the smearing effect.

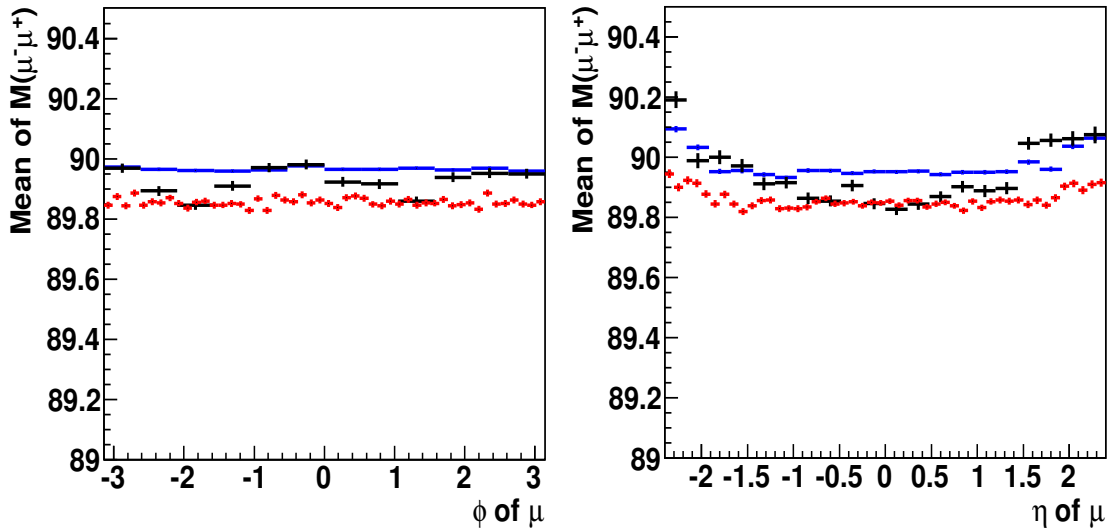


Figure 11: The $M_{\mu^+\mu^-}$ profile plot as a function of ϕ (left) and η (right) of μ (no charge requirement) after applying the the iteration 1 muon momentum additive correction.

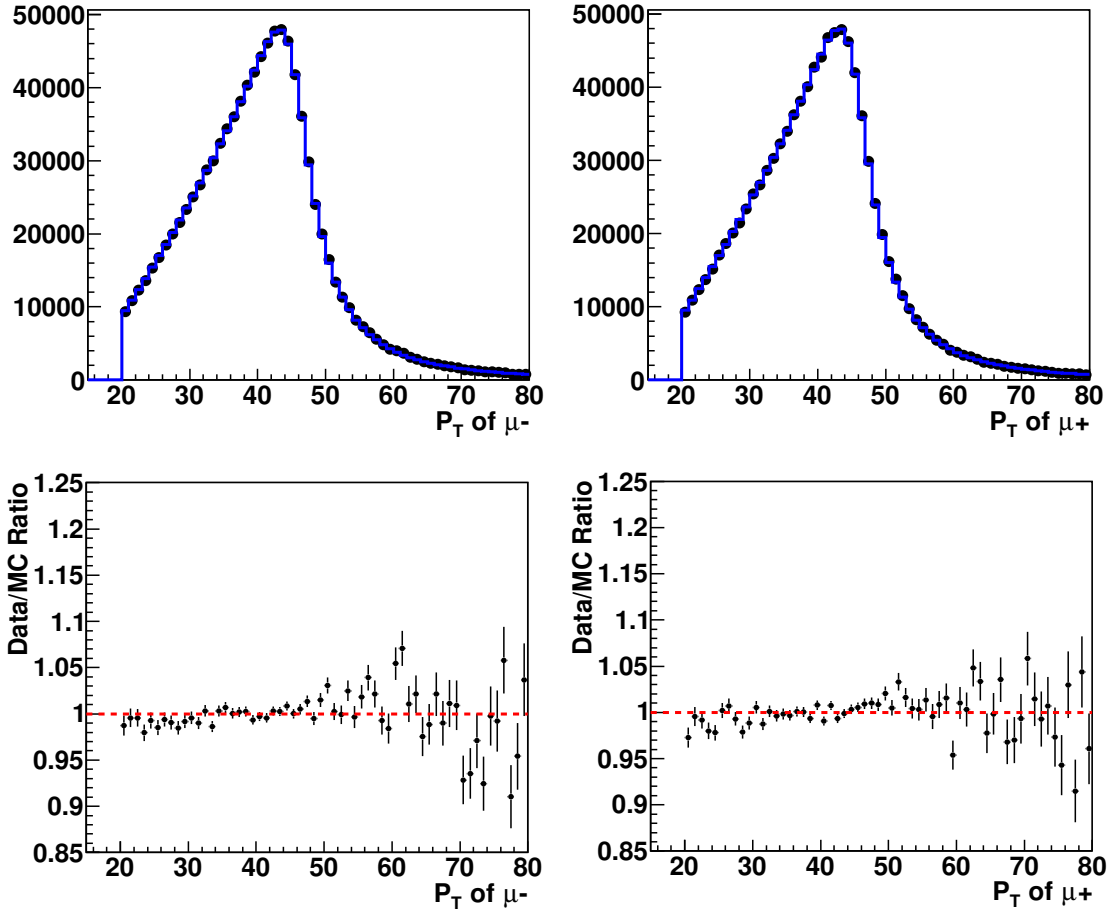


Figure 12: Iteration 1: The muon p_T spectrum in the data and MC and its ratio after applying iteration 1 muon additive momentum correction and $Z P_T$ correction. Top Plots: Comparison of the p_T distribution between the data (black) and MC (blue) for μ^- (left) and μ^+ (right) after applying iteration 1 muon additive momentum correction and $Z P_T$ correction. Bottom plots: The ratio of muon p_T distribution for μ^- (left) and μ^+ (right) The plots are normalized to the total number of events of the data in $60 < M_{\mu\mu} < 120 \text{ GeV}/c^2$.

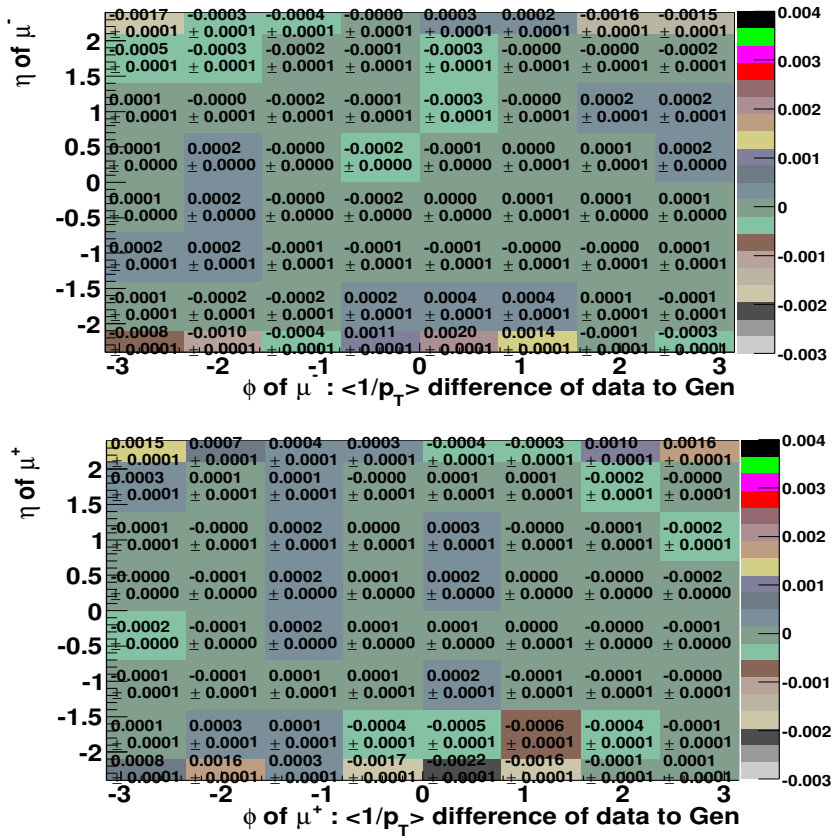


Figure 13: Final Iteration: The $\langle 1/p_T \rangle$ correction for data for μ^- (top) and μ^+ (bottom) in η and ϕ (for iteration 2).

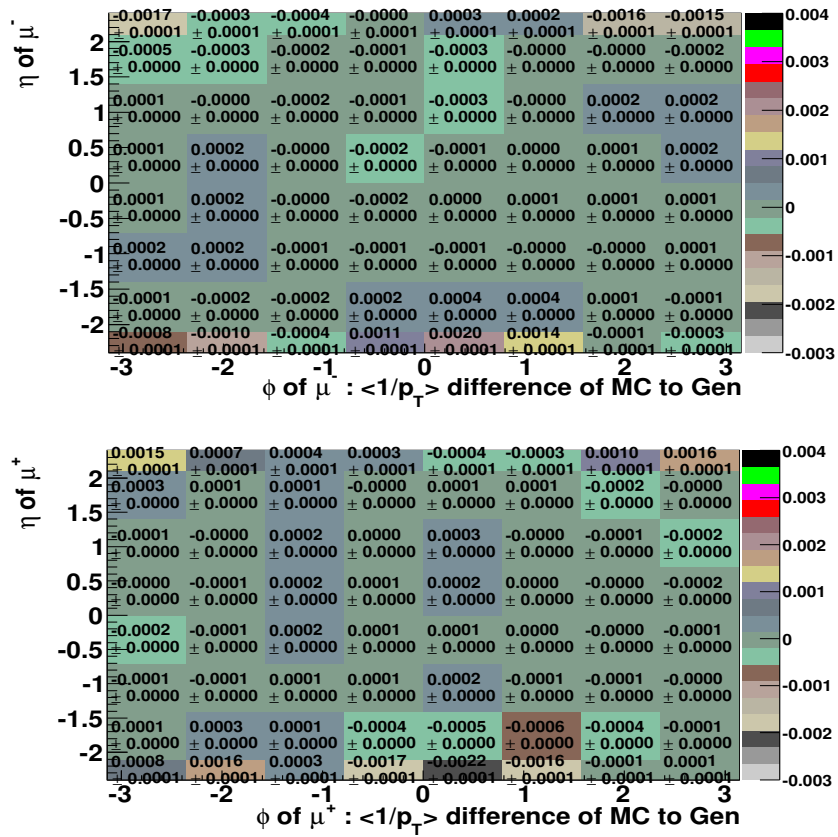


Figure 14: Final Iteration: The $\langle 1/p_T \rangle$ correction for MC for μ^- (top) and μ^+ (bottom) in η and ϕ (for iteration 2).

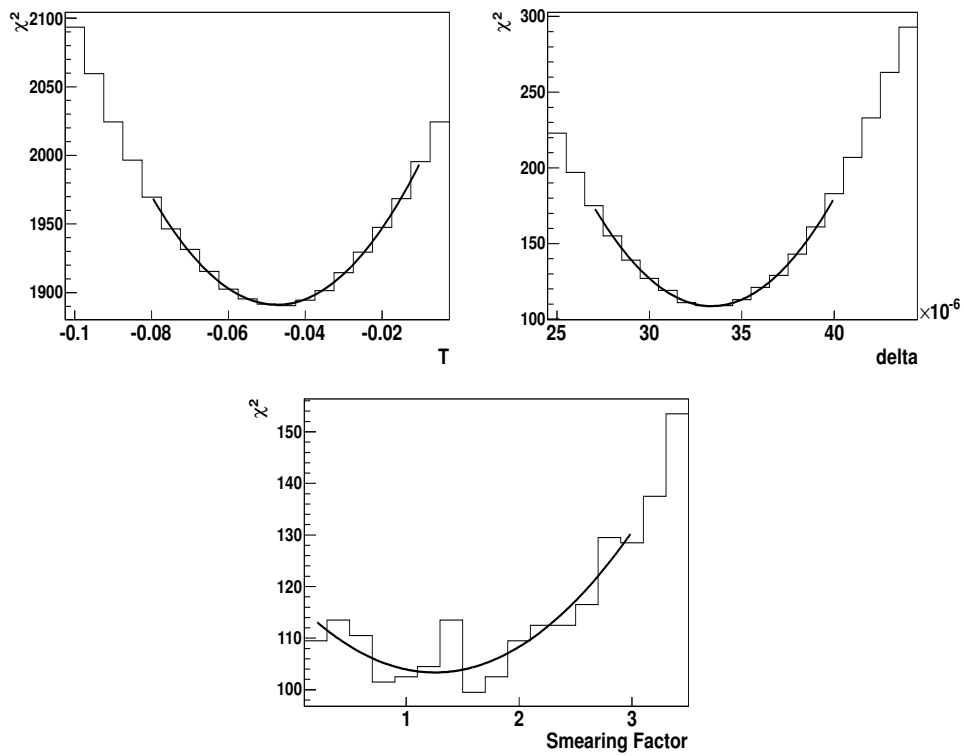


Figure 15: Final Iteration: Top Plots: χ^2 distribution as a function of the global factor, T (left) and Δ (right) (for iteration 2). Bottom Plots: χ^2 distribution as a function of the global factor, SF (for iteration 2).

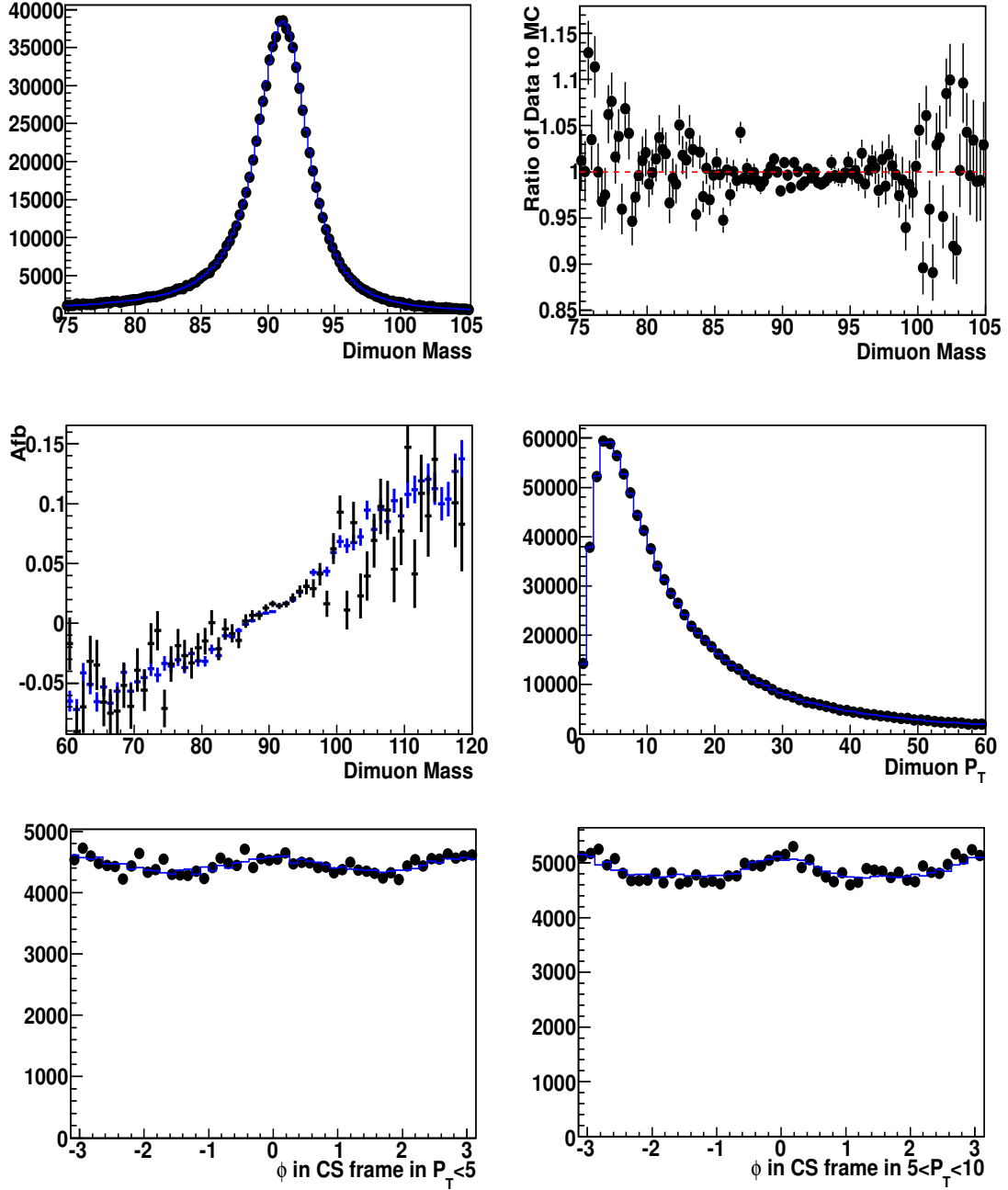


Figure 16: Final iteration: The reference plots ($M_{\mu^+\mu^-}$, A_{fb} , $Z P_T$, and ϕ_{CS}) after the application of the iteration 2 additive muon momentum correction. Top Plots: Comparison of the dimuon invariant mass distribution between the data (black) and MC (blue) (left) and its ratio of data to MC (right). Middle plots: Comparison of A_{fb} (left) and boson P_T (right) distributions between the data (black) and MC (blue). Bottom plots: Comparison of ϕ in the Collins-Soper frame in boson $P_T < 5$ GeV/c (left) and ϕ in the Collins-Soper frame in boson $5 < P_T < 10$ GeV/c (right) distributions between the data (black) and MC (blue). The plots are normalized to the total number of events of the data in $60 < M_{\mu\mu} < 120$ GeV/c².

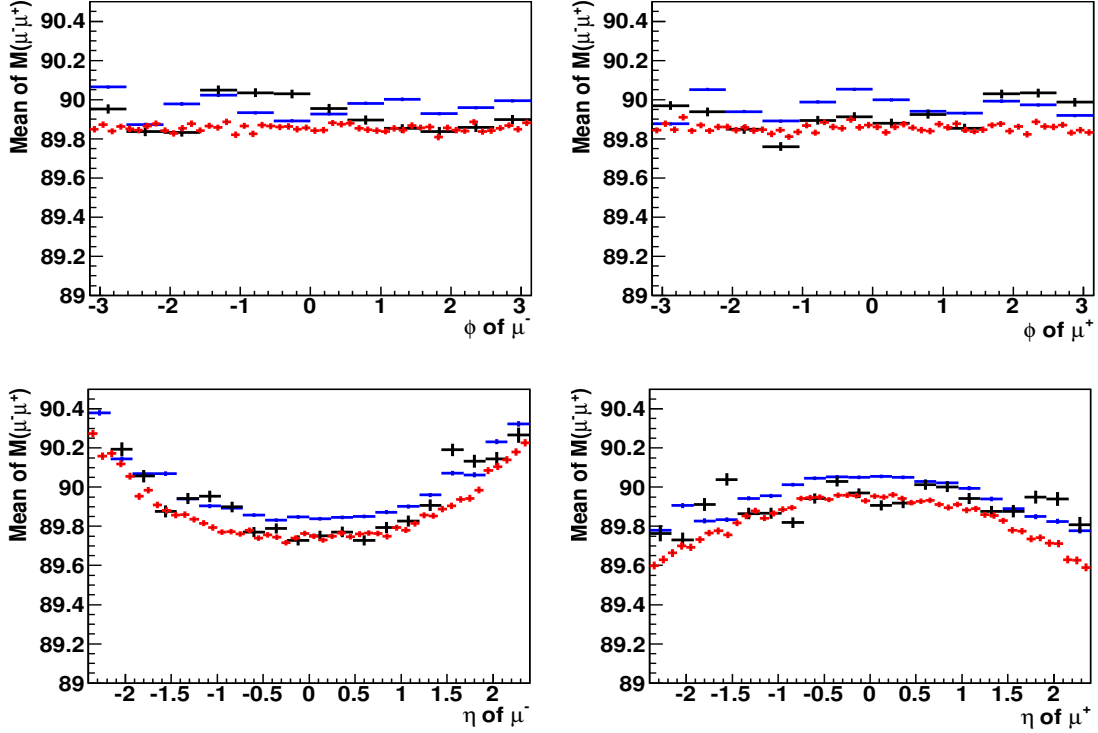


Figure 17: Final iteration: The $M_{\mu^+\mu^-}$ profile plot as a function of η and ϕ of μ^+ and μ^- after the iteration 2 muon additive momentum correction. Top Plots: Comparison of the average of $M_{\mu\mu}$ in ϕ of μ^- (left) and the average of $M_{\mu\mu}$ in ϕ of μ^+ (right) between the data (black) and MC (blue). Bottom Plots: Comparison of the average of $M_{\mu\mu}$ in η of μ^- (left) and the average of $M_{\mu\mu}$ in η of μ^+ (right) between the data (black) and MC (blue). The red points are the $M_{\mu\mu}$ profile plot as a function of ϕ and η for μ^+ and μ^- .

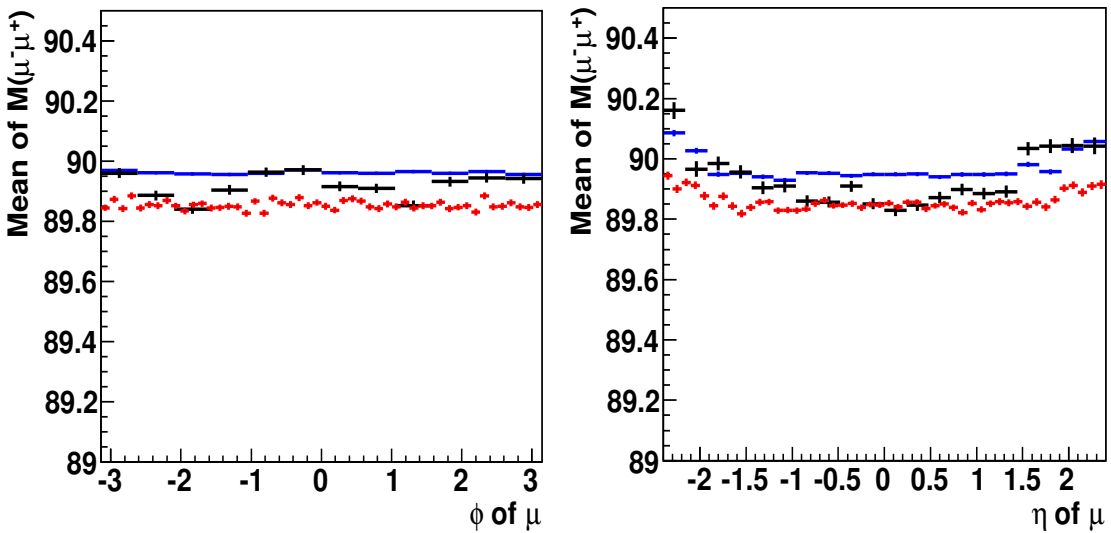


Figure 18: The $M_{\mu^+\mu^-}$ profile plot as a function of ϕ (left) and η (right) of μ (no charge requirement) after applying the the iteration 2 muon momentum additive correction.

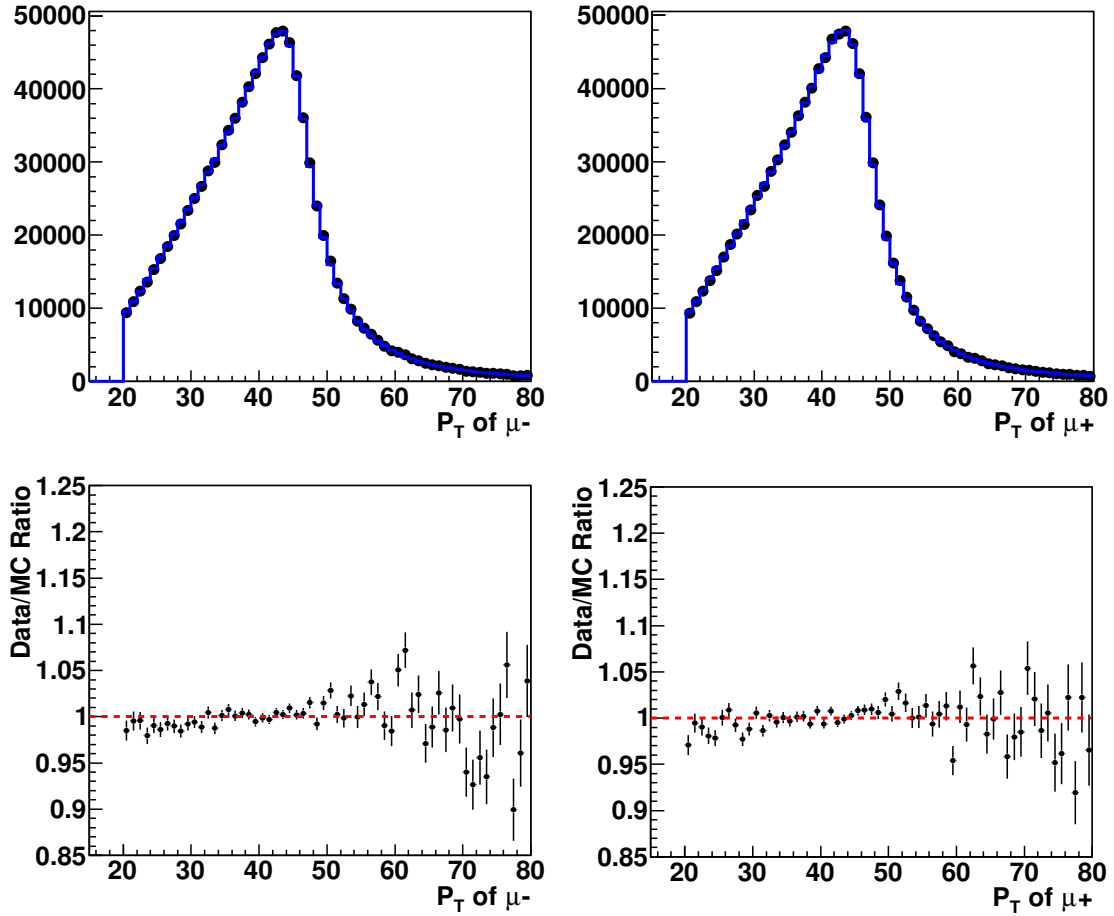


Figure 19: The muon p_T spectrum in the data and MC and its ratio after muon iteration 1 additive momentum correction and Z P_T correction. Top Plots: Comparison of the p_T distribution between the data (black) and MC (blue) for μ^- (left) and μ^+ (right) after the iteration 1 muon additive momentum correction and Z P_T correction. Bottom plots: The ratio of muon p_T distribution for μ^- (left) and μ^+ (right) The plots are normalized to the total number of events of the data in $60 < M_{\mu\mu} < 120 \text{ GeV}/c^2$.

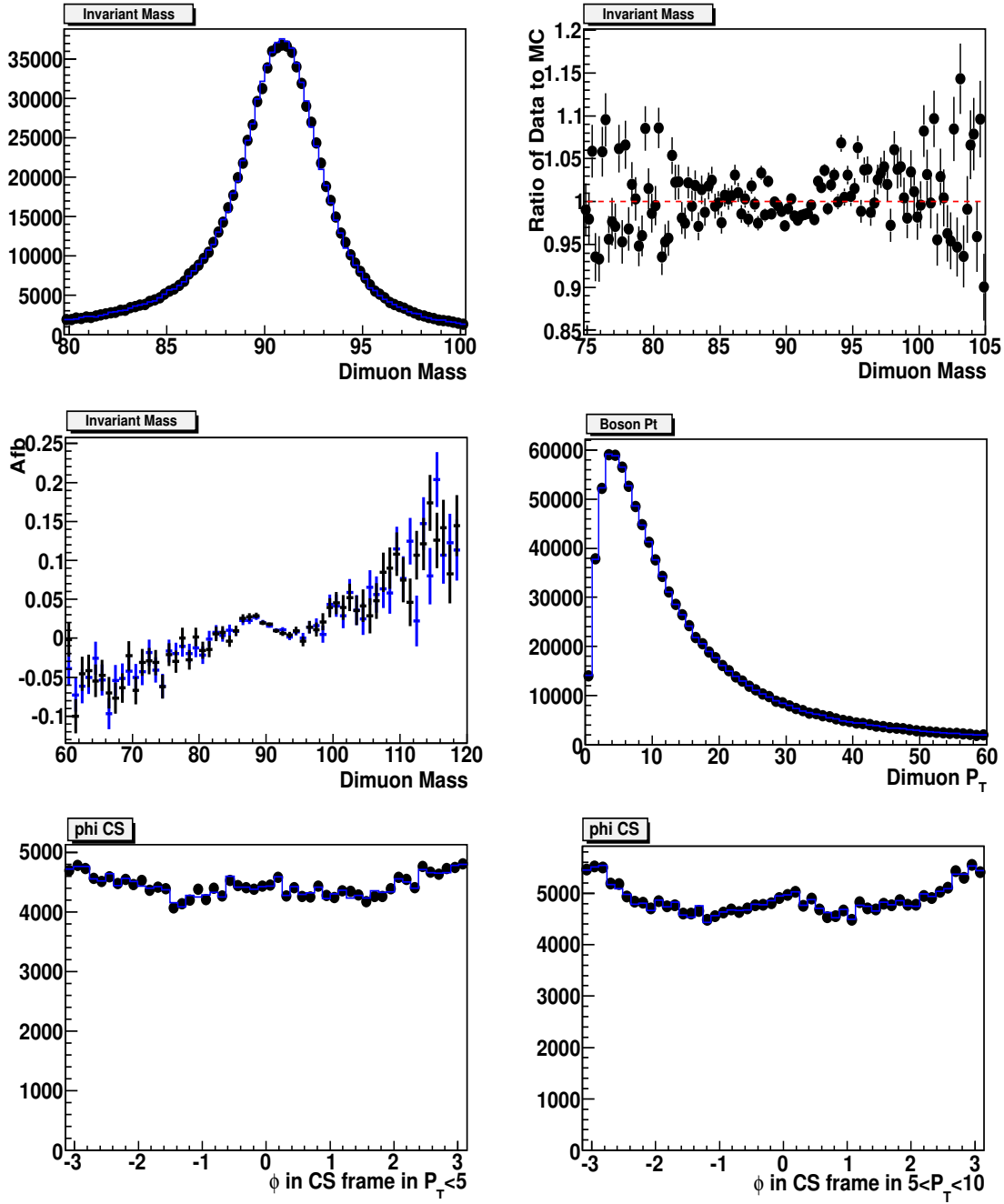


Figure 20: MuscleFit test for data: The effect of the MuscleFit correction (for the first 1/3 of the 2011A data) when applied to the full 2011A data. Top Plots: Comparison of the dimuon invariant mass distribution before (black) and after (blue) applying MuscleFit (left) and its ratio (right). Middle plots: Comparison of A_{fb} (left) and boson P_T (right) distributions before (black) and after (blue) applying MuscleFit correction. Bottom plots: Comparison of ϕ in the Collins-Soper frame in boson $P_T < 5 \text{ GeV}/c$ (left) and ϕ in the Collins-Soper frame in boson $5 < P_T < 10 \text{ GeV}/c$ (right) distributions before (black) after (blue) applying the MuscleFit correction.

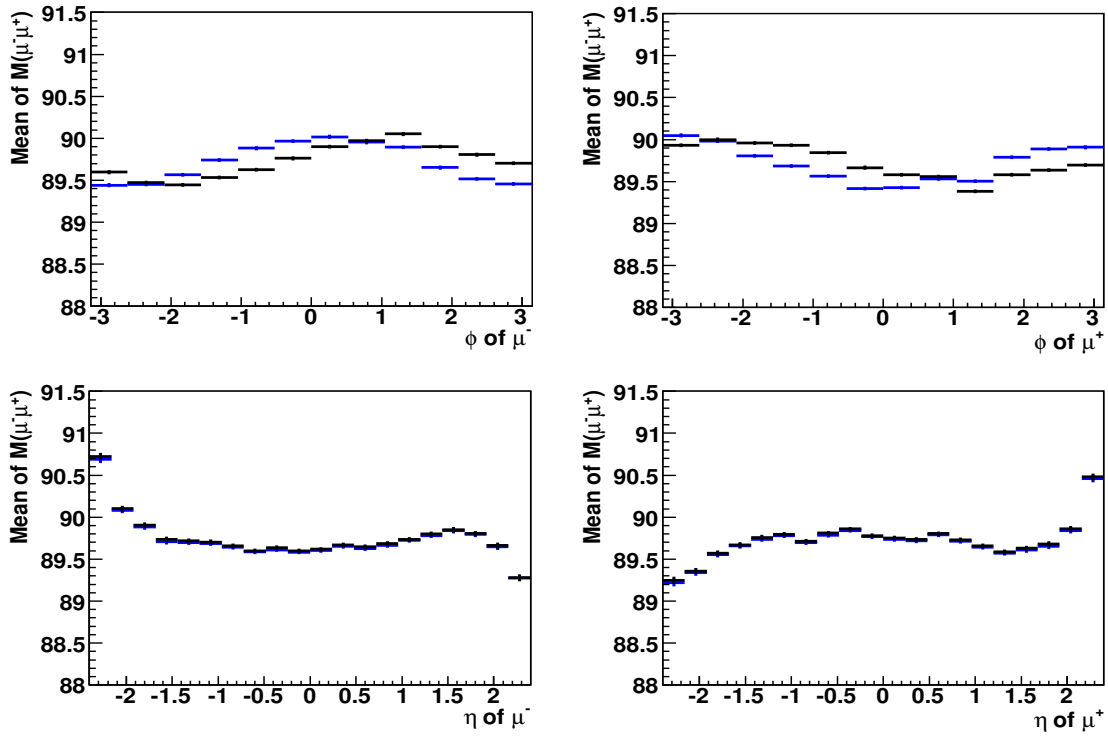


Figure 21: MuscleFit test for data: The effect of the MuscleFit correction (for the first 1/3 of the 2011A data) when applied to the full 2011A data. Top Plots: Comparison of the average of $M_{\mu\mu}$ as a function of ϕ for μ^- (left) and the average of $M_{\mu\mu}$ as function of ϕ for μ^+ (right) before (black) and after (blue) applying the MuscleFit correction. Bottom Plots: Comparison of the average of $M_{\mu\mu}$ as a function of η for μ^- (left) and the average of $M_{\mu\mu}$ as a function of η for μ^+ (right) before (black) and after (blue) applying the MuscleFit correction.

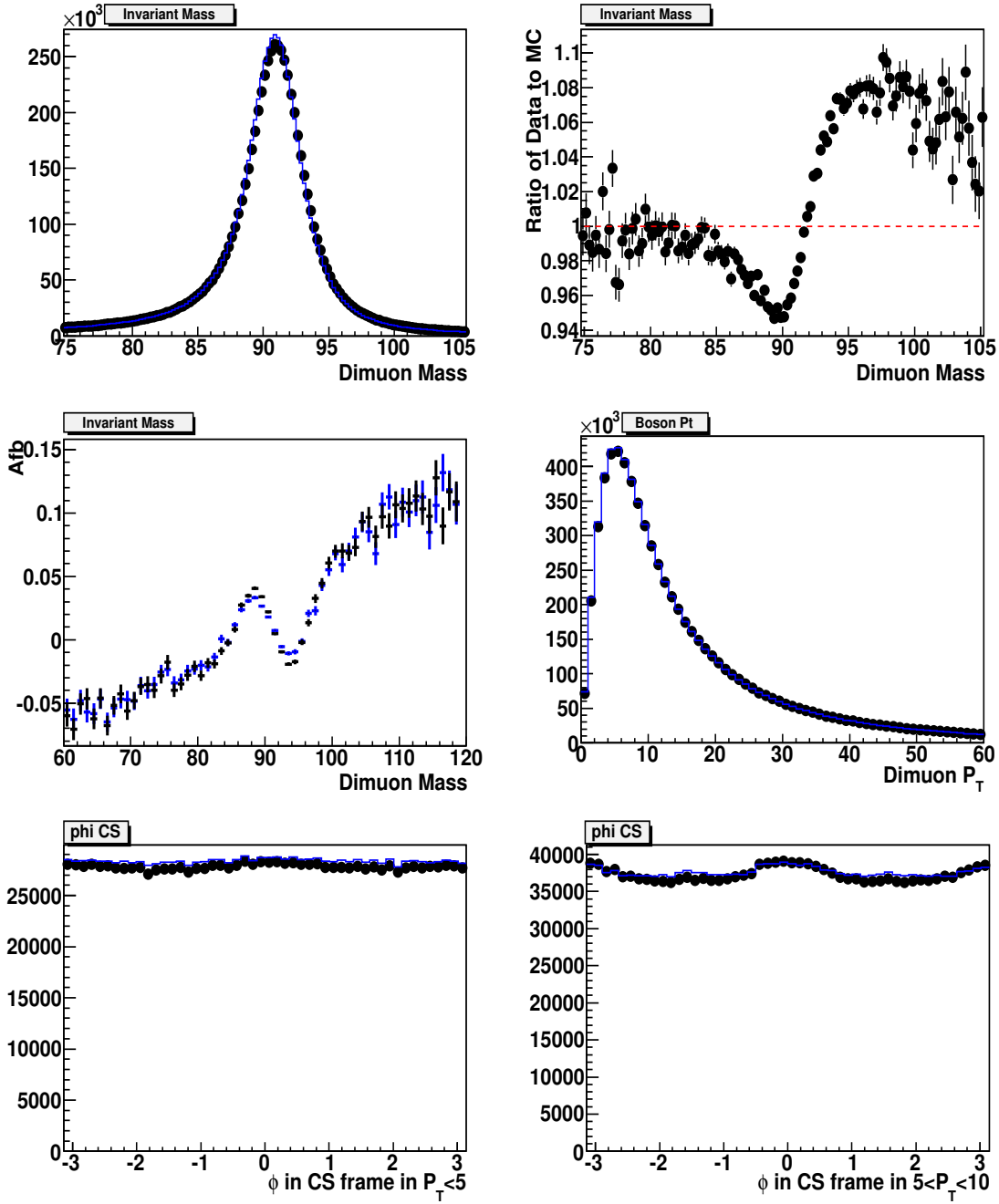


Figure 22: MuscleFit test for MC: The effect of using the MuscleFit for the 2010 MC on the 2011A MC sample. Top Plots: Comparison of the dimuon invariant mass distribution before (black) and after (blue) applying MuscleFit (left) and its ratio (right). Middle plots: Comparison of A_{fb} (left) and boson P_T (right) distributions before (black) and after (blue) applying the 2010 MC MuscleFit correction. Bottom plots: Comparison of ϕ in the Collins-Soper frame in boson $P_T < 5 \text{ GeV}/c$ (left) and ϕ in the Collins-Soper frame in boson $5 < P_T < 10 \text{ GeV}/c$ (right) distributions before (black) after (blue) applying the 2010 MC MuscleFit correction.

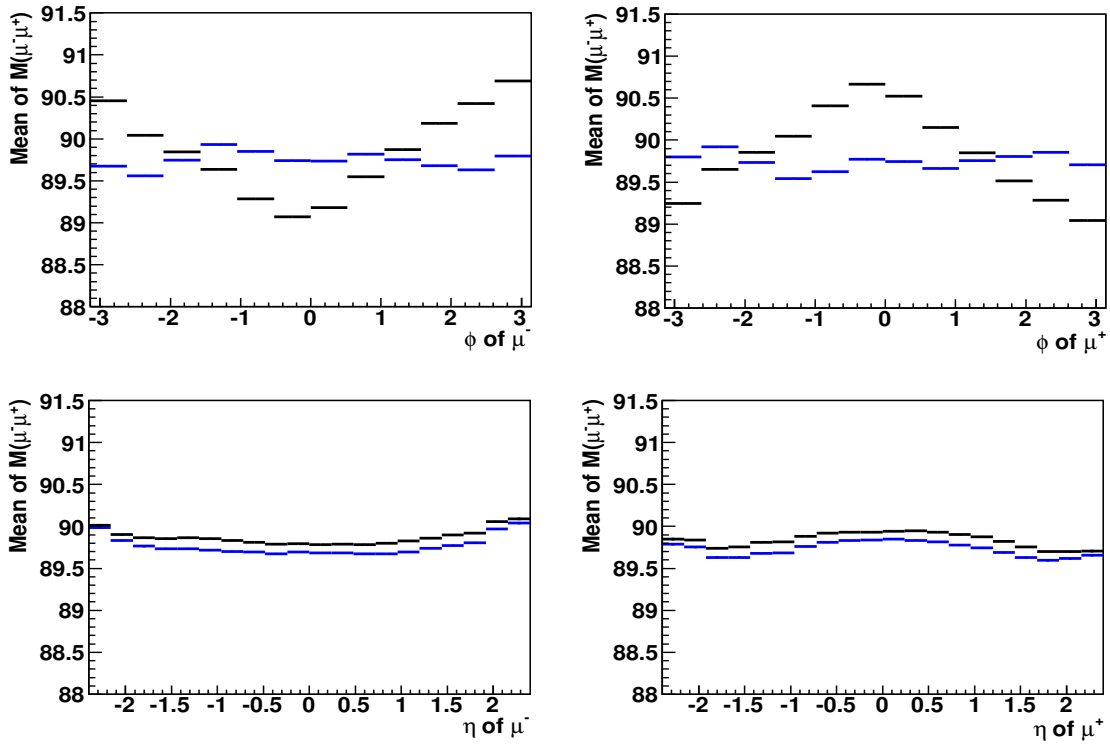


Figure 23: MuscleFit test for MC: The effect of using the MuscleFit for the 2010 MC on the 2011A MC sample. Top Plots: Comparison of the dimuon invariant mass distribution before (black) and after (blue) applying MuscleFit (left) and its ratio (right). Middle plots: Comparison of A_{fb} (left) and boson P_T (right) distributions before (black) and after (blue) applying the 2010 MC MuscleFit correction. Bottom plots: Comparison of ϕ in the Collins-Soper frame in boson $P_T < 5 \text{ GeV}/c$ (left) and ϕ in the Collins-Soper frame in boson $5 < P_T < 10 \text{ GeV}/c$ (right) distributions before (black) after (blue) applying the 2010 MC MuscleFit correction.

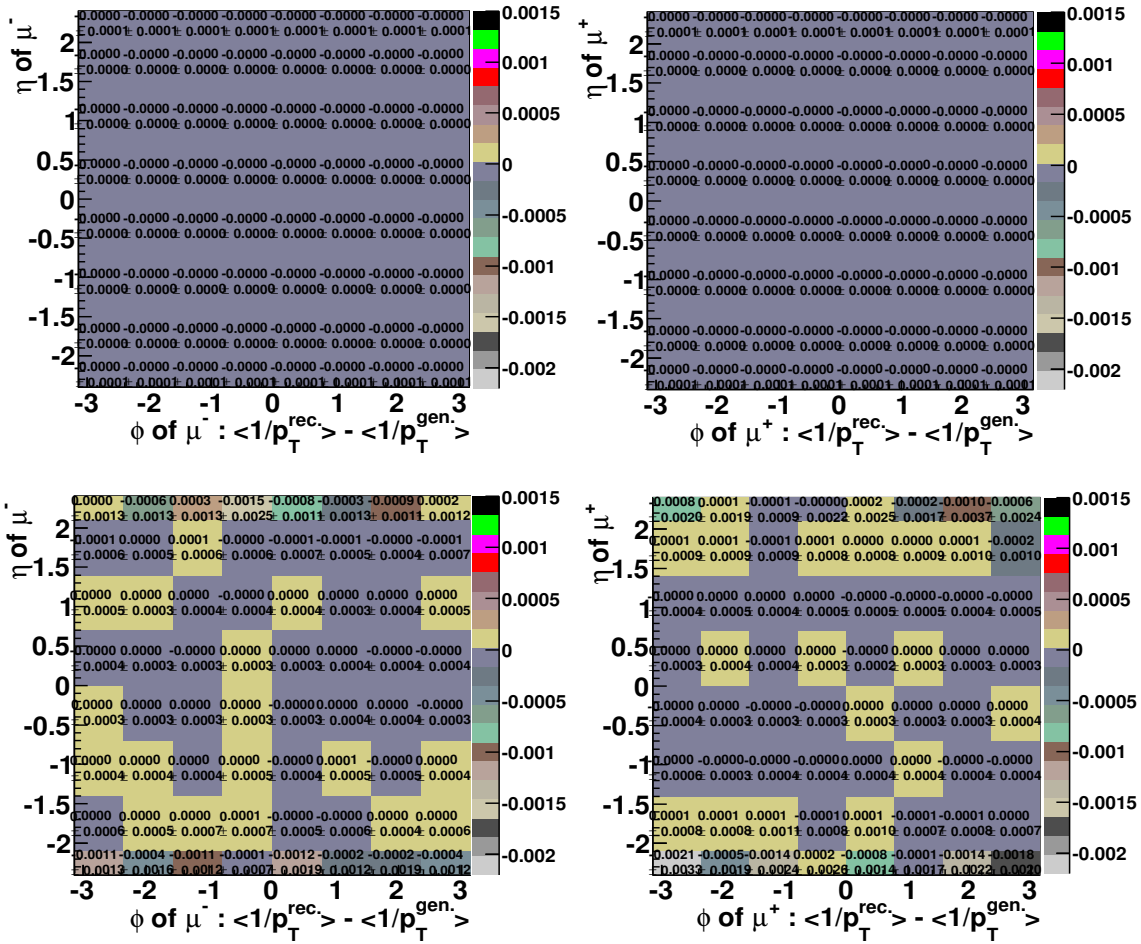


Figure 24: MC test of the muon momentum correction at Z mass and the high mass: The difference of $\langle 1/p_T(rec.) \rangle$ and $\langle 1/p_T(gen.) \rangle$ in $60 < M_{\mu^+\mu^-} < 120 \text{ GeV}/c^2$ and $M_{\mu^+\mu^-} > 250 \text{ GeV}/c^2$. Top plot: The difference of $\langle 1/p_T(rec.) \rangle$ and $\langle 1/p_T(gen.) \rangle$ after applying the muon momentum correction (iteration 2) for μ^- (left) and μ^+ (right) in Z mass region, $60 < M_{\mu^+\mu^-} < 120 \text{ GeV}/c^2$. Bottom plot: The difference of $\langle 1/p_T(rec.) \rangle$ and $\langle 1/p_T(gen.) \rangle$ after applying the muon momentum correction (iteration 2) for μ^- (left) and μ^+ (right) in the high mass region, $M_{\mu^+\mu^-} > 250 \text{ GeV}/c^2$.